



## Electrodeposition of nickel from alkaline $\text{NH}_4\text{OH}/\text{NH}_4\text{Cl}$ buffer solutions

Piotr M. SKITAŁ, Przemysław T. SANECKI, Dorota SALETNIK, Jan KALEMBKIEWICZ

Faculty of Chemistry, Rzeszów University of Technology, 35-959 Rzeszów, Poland

Received 2 March 2018; accepted 28 June 2018

**Abstract:** The electrodeposition of nickel on steel and copper from alkaline  $\text{NH}_4\text{OH}/\text{NH}_4\text{Cl}$  buffer solutions was investigated by cyclic voltammetry (CV), chronopotentiometry (CP), chronoamperometry (CA) as well as an opto-digital microscope, glow-discharge optical emission spectroscopy (GD-OES), XRF, and SEM-EDS techniques. The aim was to obtain Ni coatings from weak alkaline solutions and to optimize the process. The electrolyte composition, pH, temperature as well as current and potential parameters of the process were optimized using the quality of Ni deposit as a criterion. The role of hydrogen evolution in the process was discussed. An influence of Co as an additive was also investigated. It was found that a small amount of Co catalyzes Ni deposition process and improves the quality and color of the deposit. Therefore, in the possible application, the Ni/Co codeposition should be seriously considered. It was also shown that for constant current deposition mode, the width of self-established potential range, revealed at the very beginning of the process by the chronopotentiometric  $E=f(t)$  curves, is related to the quality of the coating.

**Key words:** nickel; cobalt; electrodeposition; ammonia buffer solution

### 1 Introduction

Nickel electrodeposition is a very important process due to its widely practical application for technical, protective and decorative purposes. Generally, classic Watts type acidic baths at pH of 4.7–5, described in many papers e.g. [1–6], are used for bright, semi-bright and matt nickel plating. Moreover, a number of papers described the respective codeposition: Ni/Co [7–11], Ni/Zn [12,13], Ni/Fe [14], Ni/Cr [15], Ni/Al [16], Co/Ni/Fe [17], Ni/TiO<sub>2</sub> [18] and Ni/TiN [19] codeposition. The nickel deposition is connected with hydrogen evolution since the process is catalyzed by the presence of metallic nickel [9]. The presence of chloride anions is required to maintain a constant concentration of Ni<sup>2+</sup> cations by means of nickel anode dissolution.

The advantages of Watts type acidic baths probably made a situation, where an alternative is rarely sought. Their problem is the hydrogen evolution and the associated decrease in current efficiency and metal surface hydrogenation [20]. Nevertheless, attempts to apply slightly alkaline solutions were described in Refs. [21–23] and the limitation of hydrogen evolution was raised as an advantage. In contrast to acidic baths,

the application of alkali ones was the interest of a very few papers for Ni deposition alone [21–23] and Ni/Zn codeposition [24]. ZHENG et al [21] focused on obtaining black nickel on RuO<sub>2</sub>/Ti electrode. ZHENG et al [22] investigated testing of nickel electroplating in a solution containing ammonia and chloride without sulfate ions. The quality of the coatings and their possible usefulness were not investigated, and the focus was to achieve high current efficiency. GRUJICIC and PESIC [23] focused on the examination of the mechanism realized at vitreous carbon electrode by cyclic voltammetry (CV) method and not on obtaining nickel coatings.

Currently, there are no complete data to estimate the possibility of mildly alkaline solutions industrial application. In respective patents [25–28], mainly the series of brighteners for such mildly alkaline nickel plating solutions are described. Therefore, in the present work, to assess the value of nickel deposition process from ammonia alkaline solutions, the process was investigated and optimized by the selection of bath composition, pH, current density, potential, temperature as well as the codeposition with cobalt. The properties of obtained deposits were compared with those obtained by using classical Watts baths.

## 2 Experimental

### 2.1 Apparatus

The (chronopotentiometry) (CP), cyclic voltammetry CV, chronoamperometry (CA) experiments were carried out by means of PGSTAT100 potentiostat/galvanostat with high current module BOOSTER10A (AUTOLAB). All potentials are related to SCE (saturated calomel electrode) reference electrode. The reference electrode was placed in the investigated solution. Its temperature was the same as that of the bath. The potential of the SCE at 40 °C, in which most experiments were done, was assumed as a standard (0.234 V). The potential of SCE at other temperatures (20, 30, 50 and 60 °C) was recalculated to this standard. The difference of 20 °C corresponds to potential value of 13.4 mV (−0.67 mV/°C). Microscopic images, as well as the surface roughness of the samples, were recorded by means of DSX500i opto-digital microscope (OLYMPUS).

The samples with deposited Ni and Ni/Co coatings were investigated by GD–OES technique with the use of GDS GD PROFILER HR spectrometer and by XRF technique with the use of ARL ADVANT'XP Sequential XRF X-ray spectrometer. Electronic scanning microscope (Hitachi S–3400N) was also used in the following settings: high vacuum mode (HV), secondary electron beam detector (SE), 20 kV acceleration voltage, spot size <100 nm, magnification 5x to 300000x. Due to the high surface homogeneity, three areas were selected for each sample. Chemical composition analysis was performed by X-ray diffraction (EDS) analysis in the areas marked with a photo frame. The results of the EDS analysis are presented in the form of X-ray spectrum (qualitative analysis) and as a report of chemical element content (quantitative analysis).

### 2.2 Experimental procedures

The electrodeposition process was carried out by using baker-type electrolyzer with two Ni plate anodes and one cathode located mutually parallel. The total volume of the electrolyte was 100 mL. Electrode dimensions were 13.5 cm × 2.5 cm for both anodes and 12 cm × 2 cm for the cathode; working surface of the cathode was 14 cm<sup>2</sup> (both sides) for CP, CA experiments and 8 cm<sup>2</sup> for CV experiment. Regardless of the electrolysis current, the process was carried out until it reached the same electric charge ( $Q=336$  C); it corresponds to the theoretical Ni layer thickness of 8.2 μm. The process was carried out in the following temperature regimes: 20, 30, 40, 50 and 60 °C.

Before deposition, steel samples were electropolished for 10 min in solution: 600 mL 85% H<sub>3</sub>PO<sub>4</sub>,

370 mL 96% H<sub>2</sub>SO<sub>4</sub>, 30 mL H<sub>2</sub>O; current density 0.23 A/cm<sup>2</sup>; immersed surface of sample 24–28 cm<sup>2</sup>. The copper samples were electropolished for 10 min in solution: 700 mL 85% H<sub>3</sub>PO<sub>4</sub>, 350 mL H<sub>2</sub>O, current density 0.38 A/cm<sup>2</sup>; followed by immersing in 65% HNO<sub>3</sub> (HNO<sub>3</sub>/H<sub>2</sub>O volume ratio of 1:1) solution for 1 s.

### 2.3 Compositions of baths

Solution 1 for Ni deposition (S1) contained 0.5 mol/L NiSO<sub>4</sub>, 1 mol/L NH<sub>4</sub>OH, 0.9 mol/L (NH<sub>4</sub>)<sub>2</sub>SO<sub>4</sub>, 0.5 mol/L NH<sub>4</sub>Cl. Final pH=7.7, 8.4 or 9.4 was established with the use of NH<sub>4</sub>OH or H<sub>2</sub>SO<sub>4</sub> solution. Solution 2 for Ni deposition (S2) contained 0.5 mol/L NiSO<sub>4</sub>, 1 mol/L NH<sub>4</sub>OH, 0.9 mol/L (NH<sub>4</sub>)<sub>2</sub>SO<sub>4</sub>, 0.5 mol/L NH<sub>4</sub>Cl, 1×10<sup>−6</sup>, 10×10<sup>−6</sup>, 100×10<sup>−6</sup>, 1000×10<sup>−6</sup> and 10000×10<sup>−6</sup> C<sub>6</sub>H<sub>5</sub>SO<sub>3</sub>Na (SDS). Final pH of S2 was 8.4. Solution 3 for Ni and Co codeposition (S3) contained 0.5 mol/L NiSO<sub>4</sub>, 1 mol/L NH<sub>4</sub>OH, 0.9 mol/L (NH<sub>4</sub>)<sub>2</sub>SO<sub>4</sub>, 0.5 mol/L NH<sub>4</sub>Cl, 0.025 mol/L CoCl<sub>2</sub>·6H<sub>2</sub>O. Final pH of S3 was 8.2. The content of Ni<sup>2+</sup> in the solutions used for deposition was controlled with the use of colorimetric method at λ=360 nm and 578 nm (Hitachi 5100). The results indicate that the constant level of Ni<sup>2+</sup> is maintained, provided that the hydrogen evolution is kept under 5% of current efficiency. If the evolution of hydrogen increases, the concentration of Ni<sup>2+</sup> in the bath (2%–4%) slightly increases. During the preparation of mildly alkaline NH<sub>4</sub>OH/NH<sub>4</sub>Cl buffer solutions S1, S2 and S3 in the presence of NH<sub>4</sub>Cl, no nickel hydroxide precipitates unless pH is below 7.7. On the contrary, in the absence of NH<sub>4</sub>Cl, an addition of NH<sub>4</sub>OH into the Ni<sup>2+</sup> solution produces a precipitate which is soluble in the excess of reagent, although a small amount of Ni(OH)<sub>2</sub> remains insoluble. The electrolyte composition was controlled by spectrophotometry of Ni<sup>2+</sup> ions in solution (Ni<sup>2+</sup> concentration), pH (NH<sub>3</sub> concentration) and conductivity measurement. The evaporation of NH<sub>3</sub> was not a problem since pH did not change during the course of the experiment. Solution 4 for electroless Ni deposition (S4) contained solution 4A (0.084 mol/L NiCl<sub>2</sub>·6H<sub>2</sub>O) and solution 4B (0.24 mol/L NaH<sub>2</sub>PO<sub>2</sub>·H<sub>2</sub>O, 0.12 mol/L CH<sub>3</sub>COONa, pH=7.3). Solutions 4A and 4B were mixed at a volume ratio of 1:1. The deposition process was carried out at 90–95 °C. Watts type solution contained 58.5 g NiSO<sub>4</sub>·6H<sub>2</sub>O, 7.5 g NiCl<sub>2</sub>·6H<sub>2</sub>O and 10 g H<sub>3</sub>BO<sub>3</sub>, refilled with water to 250 mL; it corresponded to 0.89 mol/L NiSO<sub>4</sub>·6H<sub>2</sub>O, 0.13 mol/L NiCl<sub>2</sub>·6H<sub>2</sub>O and 0.65 mol/L H<sub>3</sub>BO<sub>3</sub>.

## 3 Results and discussion

### 3.1 Results of constant current electrolysis (CCE) method

The results of Ni deposition, in a form of images of

the steel/Ni samples at pH=7.7, 8.4 and 9.4, are presented in Fig. 1.

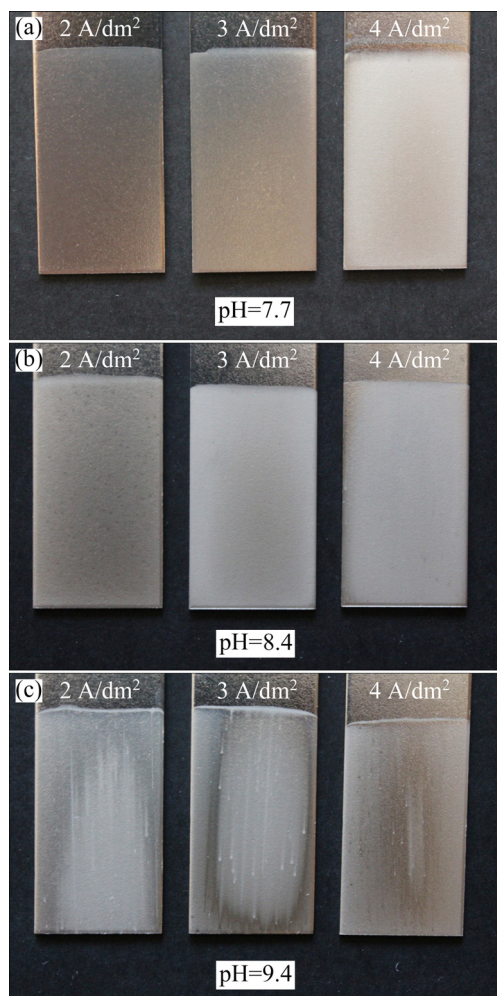


**Fig. 1** Deposition of nickel in alkaline ammonia solutions at different pH and current density values (CCE mode) (Optimization of pH and current density. Real photo of deposits obtained on Fe (steel) sample at pH=7.7, 8.4 and 9.4. At pH=7.7, a semi-bright but rough coating was obtained which was confirmed by microscopic images)

The results in Fig. 1 give important information regarding the evolution of hydrogen and the quality of the coating. Current density and pH were applied as the input variables. At pH=9.4, visible spots of thinner nickel layer are obtained. Evidently, the slow evolution of hydrogen generates its standstill (anchored) bubbles on the surface which block the surface at these points. Moreover, for samples obtained with a current efficiency less than 96% (Fig. 1, pH=8.4), where hydrogen evolution is more intensive, the effect does not occur. Generally, at any pH value, hydrogen evolution should be kept intensively enough to obtain a good quality smooth deposit without spots which can be easily regulated by current density. The hydrogen evolution reaction (HER) process is tightly linked with current

efficiency, determined from the mass of the deposited metal and respective charge exchange (Table 1). The current efficiency of the Ni deposition process with the simultaneously occurring HER was found to be relatively high in all cases including optimized conditions (pH=8.4, 3 A/dm<sup>2</sup>).

**Table 1** Current efficiencies at various pH values (Solution S1)

pH	Current efficiency/%		
	2 A/dm <sup>2</sup>	3 A/dm <sup>2</sup>	4 A/dm <sup>2</sup>
7.7	92.1	93.2	93.8
8.4	98.5	97.0	95.1
9.4	98.0	97.0	96.3

The microscopic images of the samples from Fig. 1 and Table 1 are presented in Fig. 2. The data of Fig. 1 and Table 1 allowed for the optimization of the hydrogen evolution process by setting the current density and pH. Increasing current efficiency to about 98% is associated with a decrease in the quality of the coating (Fig. 1, Table 1). Therefore, a slightly lower current efficiency had to be accepted in favor of the quality of the coating. Furthermore, Fig. 2 allowed for the evaluation of grain size and detection of possible cracks in the coating. The results also lead to the choice of pH=8.4 and current density 3 A/dm<sup>2</sup>. On the other hand, Figs. 2(c), (e), and (g) indicate the same quality of coating obtained at different pH and current density values.

Further information about the process was obtained with the use of CP technique, equivalent to constant current electrolysis (CCE). The results in Fig. 1 and, more importantly, corresponding to data in Fig. 3 indicate that deposition potential should be less negative than -1.30 V to avoid a higher contribution of hydrogen evolution and more negative than -1.23 V to keep the effective process of nickel deposition. This range of potential maintains the hydrogen evolution on a proper level. The  $E=f(t)$  plots in Fig. 3 provide relevant data on the role of potential value in applied CCE technique. Figure 3 indicates that the deposition potential range from -1.23 to -1.30 V takes place for the curves 3, 5, and 7. For curve 7, the range is relatively wide ( $\Delta E=37$  mV), which means that the consecutive layers were deposited at various potentials. In contrast, for curve 5 the whole layer was deposited in a narrow potential range ( $\Delta E=13$  mV), which corresponds to Figs. 1 and 2(e) at pH=8.4 and 3 A/dm<sup>2</sup>. Equally, curve 3 of Fig. 3 with  $\Delta E=22$  mV corresponds to Figs. 1 and Fig. 2(c) at pH=7.7 and 4 A/dm<sup>2</sup>.

The potential shift of Ni deposition towards more negative values with the increase of pH value, observed in Fig. 3, should be interpreted. The current efficiency for the simultaneously occurring hydrogen evolution

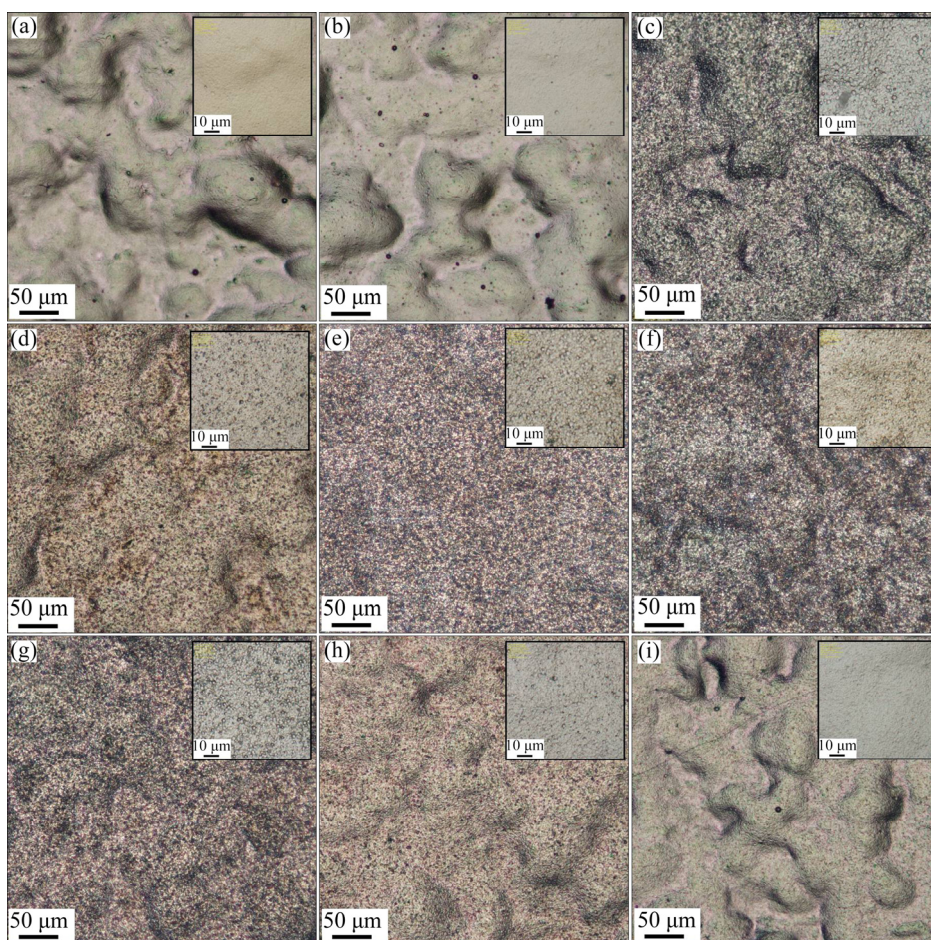


**Fig. 2** Microscopic images of samples from Fig. 1 showing comparison of various nickel layers deposited on steel at different current densities of 2 A/dm<sup>2</sup> (a, d, g), 3 A/dm<sup>2</sup> (b, e, h), and 4 A/dm<sup>2</sup> (c, f, i) and different pH values of 7.7 (a, b, c), 8.4 (d, e, f), and 9.4 (g, h, i)

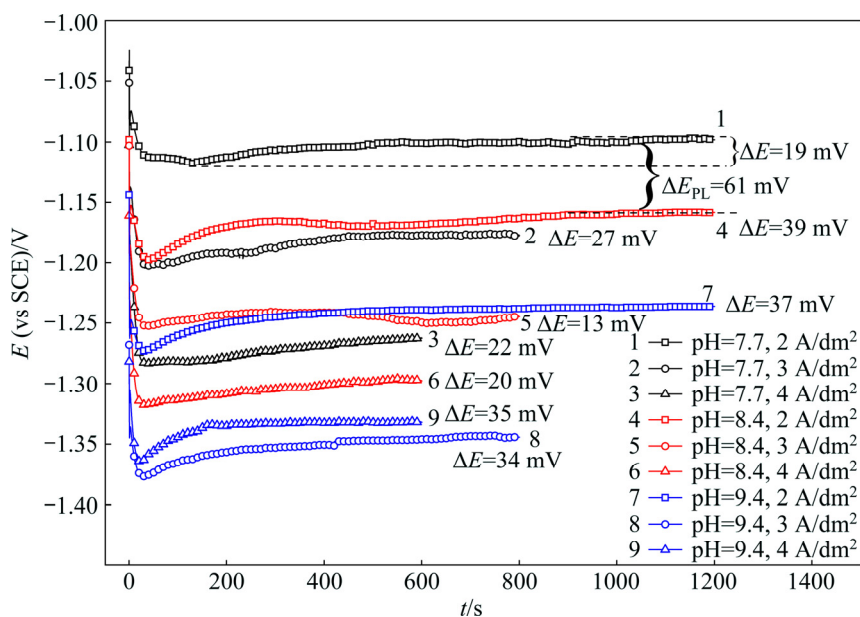


**Fig. 3** Nickel electrodeposition from alkaline solutions (CP responses at different current densities of 2, 3 and 4 A/dm<sup>2</sup> and three applied pH values of 7.7, 8.4 and 9.4. All responses correspond to nine samples shown in Figs. 1 and 2. The areas matching with clear Ni coating (Figs. 2(c), (e), (g)) corresponded to the potential range from -1.23 to -1.30 V. For all curves,  $\Delta E$  intervals were determined in the way shown for curve 1. The meaning of  $\Delta E_{PL}$  is also explained)

reaction (HER) is low in all cases (less than 8%); therefore, the influence of the HER can be neglected, at least at not very high current density. The observed trend points out the increasing complexation of  $\text{Ni}^{2+}$  ions in the solution. At pH values of 7.7, 8.4, and 9.4, the molar ratios of  $\text{Ni}/\text{NH}_3$  are approximately 1:1, 1:2, and 1:6, respectively. Therefore, decreasing this molar ratio should lead to a decrease of  $\text{Ni}^{2+}$  ions concentration. Simultaneously, a Nernstian negative potential shift  $\Delta E_{\text{PL}}$  (a shift of the current plateau) should occur, which is observed in practice. The conversion of  $\Delta E_{\text{PL}}$  parameter onto a decrease of  $\text{Ni}^{2+}$  ions concentration is shown in Table 2. Approximate  $\text{Ni}^{2+}$  concentration changes were calculated from electrochemical data namely  $\Delta E/\Delta \text{pH}$  and the Nernst equation.

On the other hand, the known values of stability constants  $\beta_1$ ,  $\beta_2$  and  $\beta_6$  for nickel complexes make it possible to estimate the values of free  $\text{Ni}^{2+}$  ion concentration. The calculation for solution S1 at pH values of 7.7, 8.4, and 9.4 gives the approximate free  $\text{Ni}^{2+}$  ion concentration values of  $1.8 \times 10^{-3}$ ,  $5.6 \times 10^{-6}$  and  $2.2 \times 10^{-12}$ , respectively. The  $\text{Ni}^{2+}$  concentration, calculated from  $\beta_1$  and  $\beta_2$ , decreased by a factor of 321. This is in consistency with the respective change calculated from electrochemical data (Table 2) where the  $\text{Ni}^{2+}$  concentration decreased by a factor of 251.

A question arises, of which ammonia complex

among possible  $\text{NiL}_n$ ,  $n=1-6$  is the dominant form in the investigated solution. For this purpose, spectral UV–Vis studies of Ni complexes were performed for solutions with different molar ratios of  $\text{Ni}/\text{NH}_3$  (Figs. 4(a) and (b)). The results indicate that starting from the molar ratio of  $\text{Ni}/\text{NH}_3$  being 1:3 and above, the positions of absorption peaks at approximately 600 and 360 nm remain constant. The green color of the solution at molar ratios of  $\text{Ni}/\text{NH}_3$  being 1:0 and 1:0.5 corresponds to  $\text{Ni}^{2+}$  aqua complex, blue color at molar ratios of  $\text{Ni}/\text{NH}_3$  being 1:1 and more corresponds to the ammonia complex. The molar ratio of  $\text{Ni}/\text{NH}_3$  being 1:2, selected as optimization for deposit quality, corresponds mainly to  $\text{NiL}_2$  complex since  $\lg \beta_1=2.75$  and  $\lg \beta_2=4.95$  [29].

On the basis of the results obtained so far (Figs. 1–3), the optimum for Ni deposition on steel consists of the bath with  $\text{pH}=8.4$ ,  $T=40^\circ\text{C}$ , current density  $3\text{ A}/\text{dm}^2$ , and the resulting current efficiency is 97%. The choice of temperature parameter should be also a result of the optimization process. The respective experimental data are presented in Fig. 5(a). The  $E=f(t)$  response of CP technique also depends on temperature (Fig. 5(b)).

Data in Fig. 5 allow for temperature optimization and suggest that  $40^\circ\text{C}$  is the best with the lowest grain size, which is in line with the early choice. Besides, the experimental results indicate that the best quality of

**Table 2** Processing of data in Fig. 3

Number of $E=f(t)$ curve from Fig. 3	Current density/ ( $\text{A} \cdot \text{dm}^{-2}$ )	$\Delta \text{pH}$	$\Delta E_{\text{PL}}/\text{mV}$	$(\Delta E_{\text{PL}}/\Delta \text{pH})/\text{mV}$	Mean value of ( $\Delta E_{\text{PL}}/\Delta \text{pH})/\text{mV}$	$(\Delta c_{\text{Ni}^{2+}}/\Delta \text{pH})/(\text{mol} \cdot \text{L}^{-1})$
1–4	2	0.7	0.061	0.087	0.082	115
4–7	2	1.0	0.078	0.078	0.082	433
2–5	3	0.7	0.071	0.101	0.099	251
5–8	3	1.0	0.097	0.097	0.099	1902
3–6	4	0.7	0.035	0.050	0.042	14.8
6–9	4	1.0	0.035	0.035	0.042	14.8

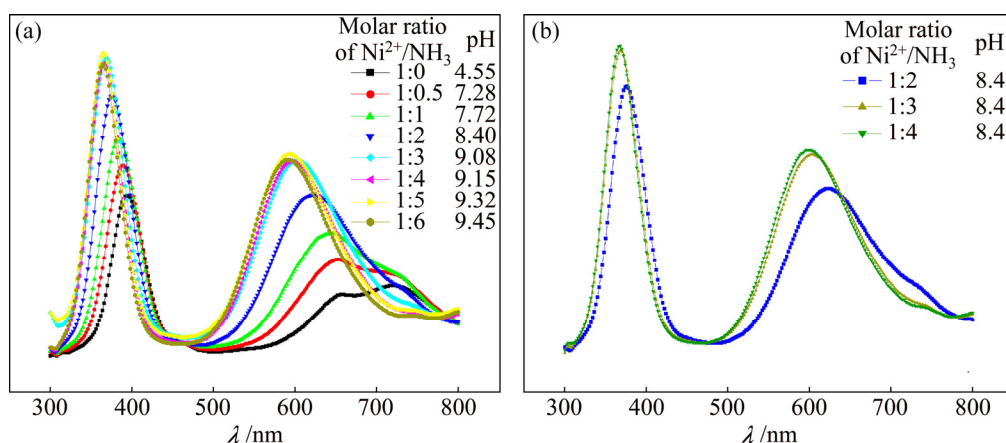


**Fig. 4** UV–Vis spectra of 0.5 mol/L  $\text{Ni}^{2+}$  in mol/L  $\text{NH}_4\text{Cl}$  solution with different molar ratios of  $\text{Ni}^{2+}/\text{NH}_3$  at different pH values (a) and optimized  $\text{pH}=8.4$  (b)

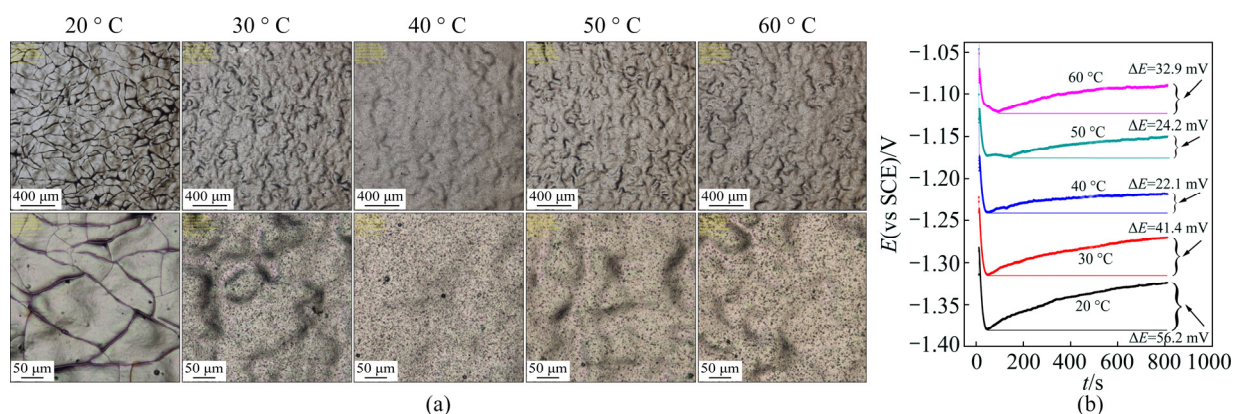


**Fig. 5** Influence of temperature on quality of electrodeposited Ni (Deposit obtained at 20 °C shows cracks) (a) and influence of temperature on Ni electrodeposition process (CP responses were obtained in optimized solution (pH=8.4, 3 A/dm<sup>2</sup>) at different temperatures; deposition technique: CCE (equivalent to CP)) (b)

deposit (Fig. 5(a)) corresponds to the narrowest  $\Delta E$  interval in  $E=f(t)$ , i.e. CP response at 40 °C (Fig. 5(b)). A cracked deposit occurs in cases when  $\Delta E$  interval is wider (Fig. 5, 20 °C). A similar conclusion was derived from results in Fig. 3. The results in Figs. 3 and 5(b) are summarized as follows: the best quality of deposits corresponds to the narrowest  $\Delta E$  interval in  $E=f(t)$  response, revealed with the use of CP technique. This experimental fact suggests that a fast potential fixing in constant current technique promotes good quality of the coating.

A comparison of Ni deposit on steel and copper is presented in Fig. 6. It is worth mentioning that the microscopic images of Ni deposit obtained on steel and copper are almost identical with that obtained by chemical electroless Ni deposition (results not shown).

The same bath and conditions are optimum for Ni deposition on a copper surface (Fig. 6).

The morphologies of the Ni coatings electrodeposited on steel and copper substrates under identical conditions are not identical (Fig. 6). Generally, in electroplating, the properties of a deposit depend on background kind, its properties, and structure.

### 3.2 Results of constant potential electrolysis (CPE) method

Figure 7 shows nickel electrodeposition from alkaline solutions by CPE at pH=8.4 and different deposition potentials and effect of potential on deposition process in solution S1 at pH=8.4. The results obtained by constant potential electrolysis (CPE), at optimized pH=8.4 (Fig. 7(b)), indicate that there exists a good relevance to the results obtained by means of constant current electrolysis (CCE). The potential value and the resulting current are responsible for the obtained structure. For small values of potential (−1.05 to −1.10 V), which correspond to low values of current

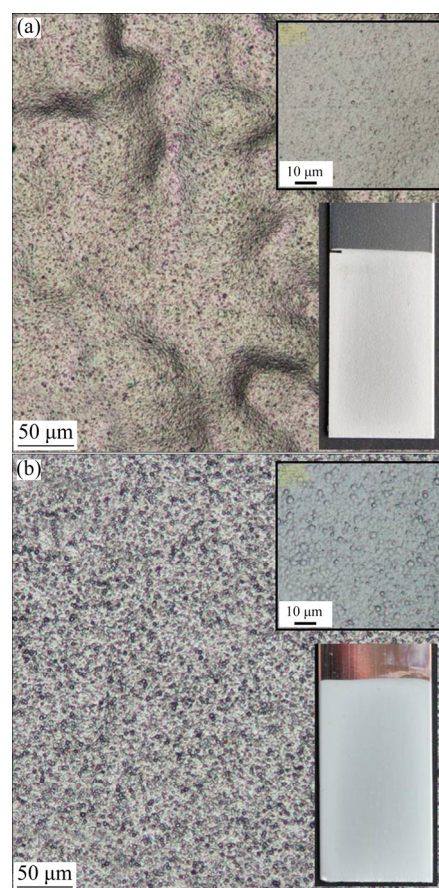


**Fig. 6** Comparison of Ni deposits on steel (a) and copper (b) at pH=8.4, 3 A/dm<sup>2</sup> in solution S1 with deposition technique of CCE

(Fig. 7(a)), bright coatings are obtained (pictures a<sub>1</sub> and b<sub>1</sub> in Fig. 7(a)). An increase of negative potential results in matte coatings (pictures d<sub>1</sub>, e<sub>1</sub> and f<sub>1</sub> in Fig. 7(a),  $E$  is from −1.23 to −1.30 V). A further shift of potential towards more intense hydrogen evolution leads to the destruction of the coatings by severe stresses and cracks (pictures g<sub>1</sub> and h<sub>1</sub> in Fig. 7(a); more negative than

–1.30 V). The constant potential electrolysis results suggest the potential range of –1.23 to –1.30 V is optimal which remains in full compliance with the results obtained indirectly by CCE method, namely –1.23 to –1.30 V (Section 3.1, Figs. 2(c), (e) and (g)).

### 3.3 Further optimization of Ni electrodeposition

To improve the quality of nickel coatings, WU et al [10] included Co as a co-deposited metal. The quoted authors reported, among others, that for 2.5% cobalt content in the coating, a silver-white layer can be obtained. The codeposition of Ni/Co alloys was also extensively investigated by VAZQUEZ-ARENAS et al [8,9]. Our results indicate that a small amount of Co ions in the bath (solution S3, 4.78% Co in the sum of Ni and Co inserted) give a brighter and smoother nickel coating. In turn, the content of Co in Ni/Co deposit, determined with the use of several spectral techniques, is 5.2%–5.8%. Current vs potential characteristics of Ni and Co are shifted relative to each other by about 160 mV at  $I=-0.4$  A (Fig. 8). Figure 8 shows that Co catalyzes nickel deposition and indirectly reduces the

hydrogen evolution. Cobalt codeposition also makes it possible to apply a higher current regime. It is worth mentioning that cyclic voltammetry (CV) deposition technique (CV electrolysis, CVE) was chosen as the best technique for the copper deposition [30,31].

To show that the additives applied to Watts type baths can also be applied for the alkaline ones, a typical additive i.e. sodium benzenesulfonate (SDS) was checked. The results (Fig. 9) indicate that the brightening effect also appears in the alkaline solution. The optimum concentration of SDS was  $1000 \times 10^{-6}$  (mass fraction). The influence of SDS concentration is also visible in CP responses (Fig. 9). Figure 9 indicates both catalytic and inhibitory effects, characteristic for the adsorption of inert organic compounds on electrodes [32].

The roughness of metallic deposit is an important parameter which was determined by using a specified option of the applied microscope. Figure 10 presents the representative results of such a determination. The roughness values of deposits were compared with those of steel and copper bases. The roughness differences between samples are significant but not high due to the

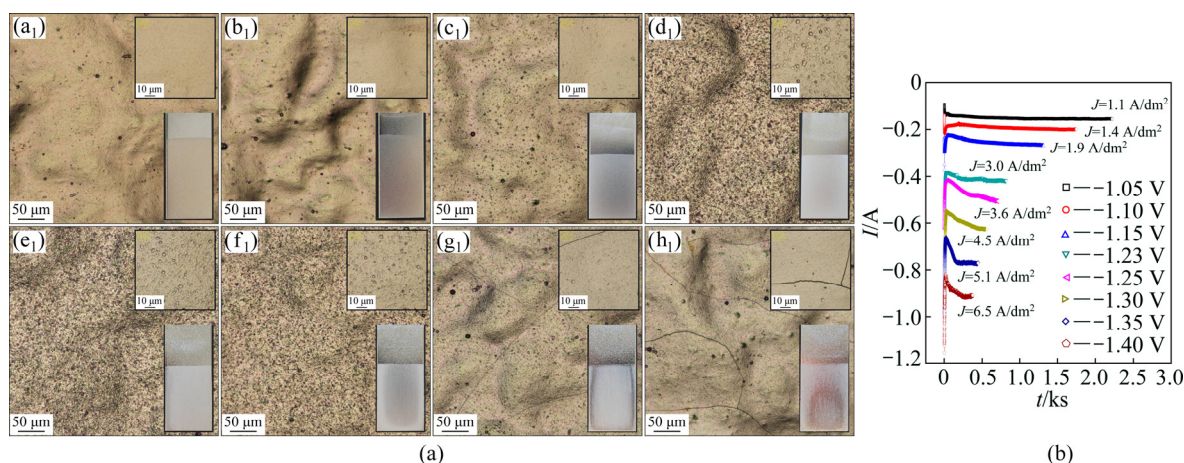


**Fig. 7** Nickel electrodeposition from alkaline solutions by CPE at pH=8.4 and deposition potentials of –1.05 V (a<sub>1</sub>), –1.10 V (b<sub>1</sub>), –1.15 V (c<sub>1</sub>), –1.23 V (d<sub>1</sub>), –1.25 V (e<sub>1</sub>), –1.30 V (f<sub>1</sub>), –1.35 V (g<sub>1</sub>) and –1.40 V (h<sub>1</sub>) (a) and effect of potential on deposition process in solution S1 at pH=8.4 (b)

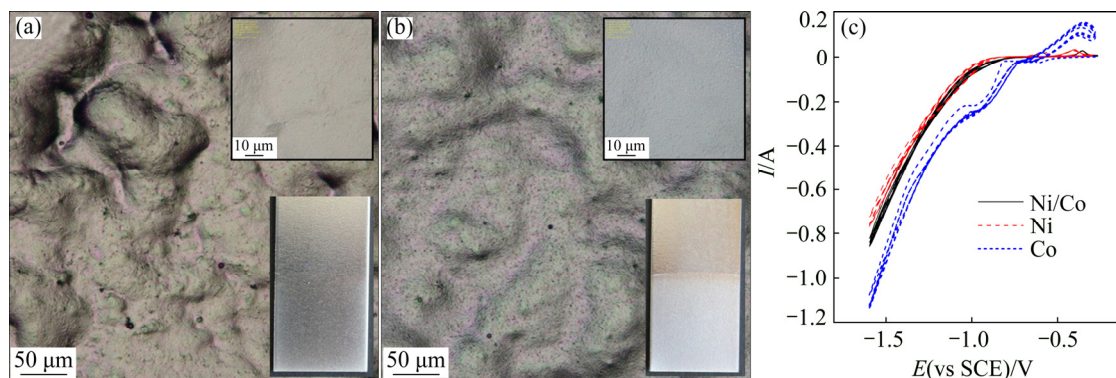


**Fig. 8** Comparison of Ni and Ni/Co deposits obtained by CVE mode: (a, b) Deposits obtained on steel with their respective microscopic images for Ni (a) and Ni/Co (b); (c) CV responses (scan rate 0.01 V/s; 4 cycles scanned to obtain  $Q=336$  C, reverse potential –1.6 V)

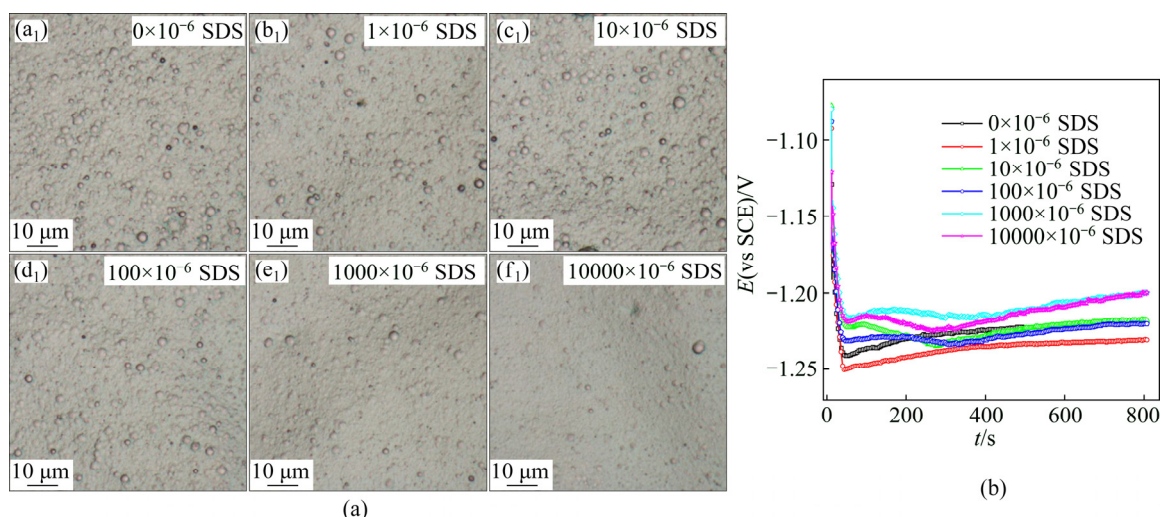


**Fig. 9** Effect of SDS concentration on microscopic image of Ni deposit (Deposition technique: CCE; solution S2; SDS concentration: 0–10000 $\times 10^{-6}$ ; current efficiency: 90%–91%) (a) and effect of SDS concentration on CP responses (Deposition technique: CCE; solution S2) (b)

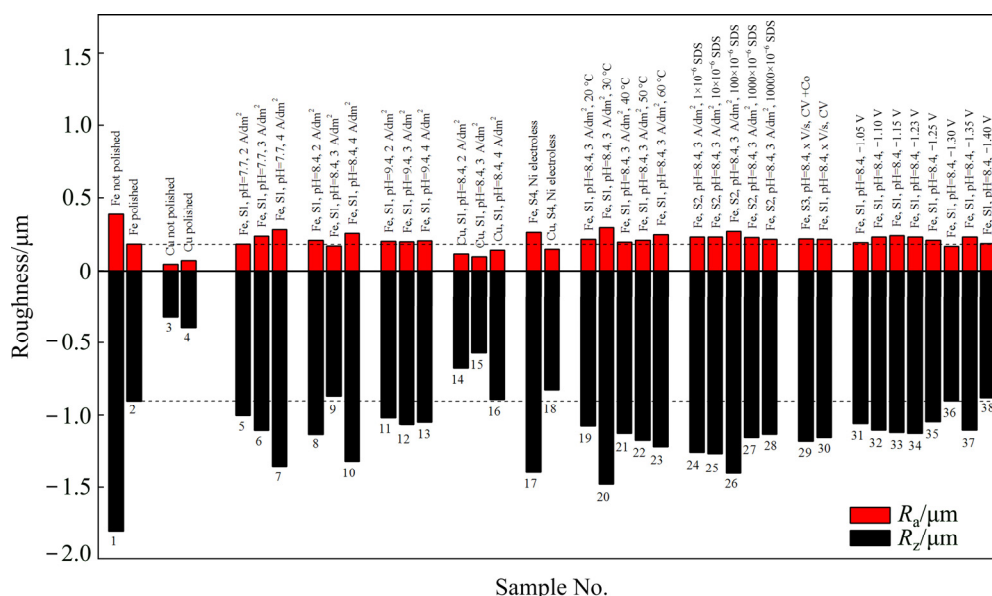


**Fig. 10** Overview of roughness describing parameters for all experimentally obtained Ni and Ni/Co deposits ( $R_a$  ( $\mu\text{m}$ ) is roughness factor: Average profile height;  $R_z$  ( $\mu\text{m}$ ) is the biggest profile height. All data were obtained and processed by using Olympus microscope. Dotted lines: Results for electropolished Fe samples before deposition)

fact that all samples were electropolished before deposition (samples 1 vs 2 and 3 vs 4) to obtain repetitive results. Moreover, the state of the metal surface also determines the quality of the coating. The results support the correctness of the presented optimization of the mildly alkaline bath since the lowest roughness results were obtained under the optimized conditions of the process (pH=8.4,  $J=3 \text{ A/dm}^2$ ,  $T=40 \text{ }^\circ\text{C}$ ). It is visible for the pairs: samples 9 vs 6 and 12 (pH criterion choice); samples 9 vs 8 and 10 (J criterion choice); samples 21 vs 19, 20 and 22, 23 (T criterion choice).

### 3.4 Composition and structure of optimized Ni and Ni/Co coatings

The compositions of Ni and Ni/Co coatings are

presented in Table 3. Three spectroscopic techniques (GD–OES, XRF, and SEM–EDS) were used to check the composition of the coatings. A confirmation of the composition was obtained for a pure Ni coating, where, depending on the technique, 100% or 96.8% Ni was determined (Table 3). The oxygen content was also determined to evaluate the degree of coating oxidation. In turn, the Ni/Co layer composition, mentioned in Section 3.3, depending on the technique, was determined as 5.2% and 5.6% of Co (GD–OES and XRF, respectively). The SEM–EDS method, based on a small surface sample, gave 7.4% of Co (Table 3). The Co content obtained by SEM–EDS method is higher in comparison to GD–OES method. The discrepancy can arise from the fact that Co peak is coupled with one of

three Fe peaks. Therefore, the most reliable Co content in the coating is 5.2%–5.6% (Table 3). Since the participation of Co in optimized bath composition is 4.78% in the sum of Ni and Co, an enrichment of the

layer in this component occurs. GD–OES technique determines not only the surface composition of the layer, but also the composition profiles along the entire deposited coating (Fig. 11). Figure 11 shows a comparison

**Table 3** Compositions of Ni and Ni/Co coatings obtained by GD–OES, XRF and EDS methods

Coating	Method	Content/%	Ni	Co	O	Fe
Ni	GD–OES*	at.	99.9	<0.1	–	<0.1
	XRF	wt.	100	0	–	–
	SEM–EDS**	wt.	96.8±0.4	0	1.1±0.1	2.1±0.1
	SEM–EDS**	at.	93.9±0.4	0	3.9±0.3	2.2±0.1
Ni/Co	GD–OES*	at.	94.7	5.2±0.2	–	<0.1
	XRF	wt.	94.2	5.6±0.2	–	–
	SEM–EDS**	wt.	90.2±0.5	7.4±0.2	1.5±0.1	0.9±0.1
	SEM–EDS**	at.	86.7±0.5	7.0±0.2	5.3±0.2	0.9±0.1

\* Measurements completed on surface of 19.6 mm<sup>2</sup>, \*\* measurements completed on surface of 0.1 mm<sup>2</sup>

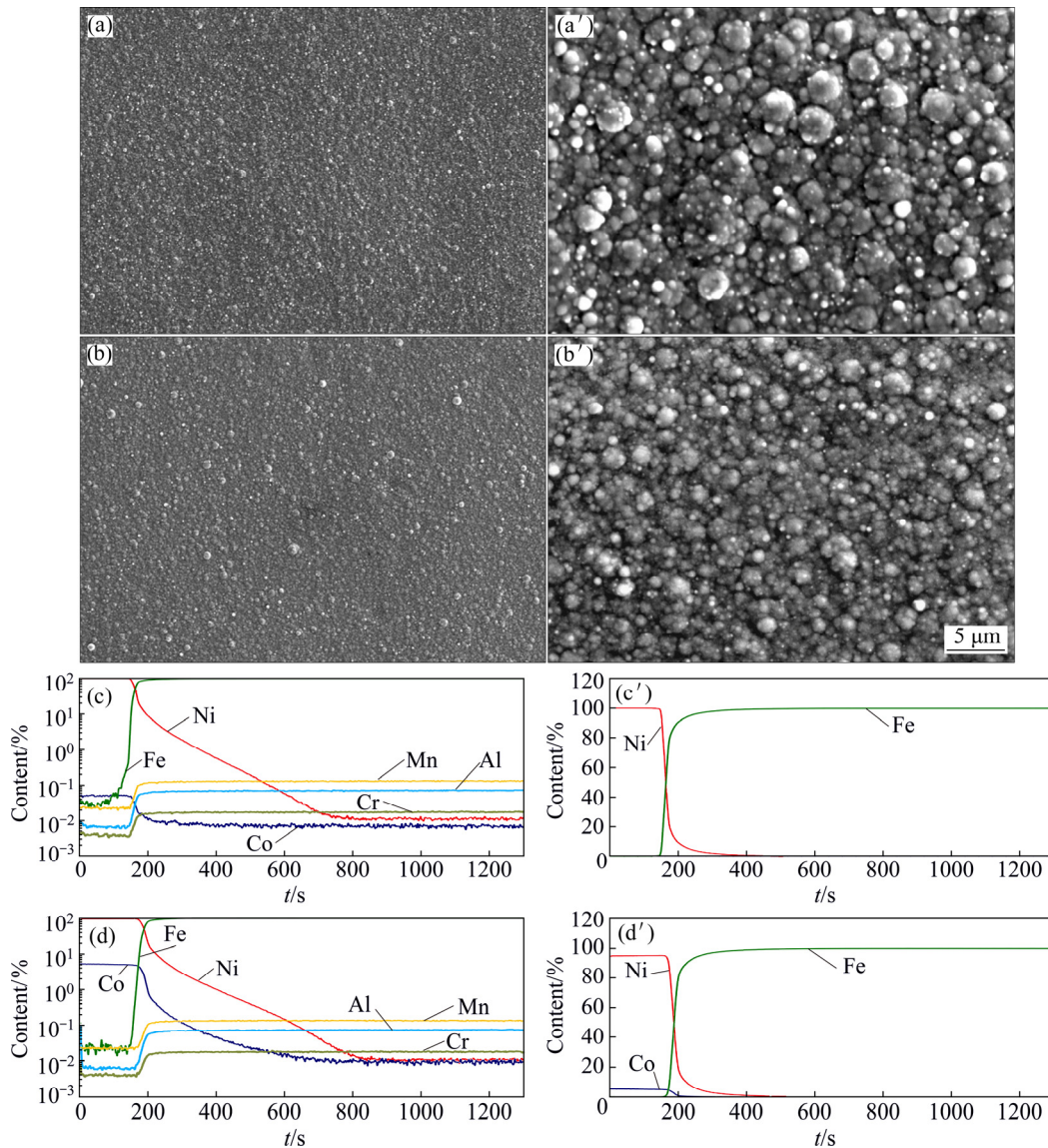


**Fig. 11** SEM images of optimized Ni (a, a') and Ni/Co (b, b') coatings, and GD–OES content (at.%) profiles of optimized Ni (c, c') and Ni/Co (d, d') coatings (Logarithmic (c, d) and linear (c', d') scales were applied. Evaporation time (x-axis) is proportional to depth of metal layer)

of the surfaces of pure Ni and Ni/Co coatings and images were recorded with SEM.

## 4 Conclusions

(1) The optimized conditions for Ni plating in ammonia alkaline solution are as follows: composition of solutions S1 or S3; temperature 40 °C; potential from  $-1.23$  to  $-1.30$  V (vs SCE); current density 3–4 A/dm<sup>2</sup>; mode of the process: CCE, CPE as well as CVE repeated run after run. The small addition of cobalt ions catalyzes the deposition of nickel and improves the quality of the coating.

(2) Even in mildly alkaline ammonia solution, the hydrogen evolution reaction (HER) due to the electrocatalytic effect of Ni deposit is present. Moreover, a noticeable contribution (up to 5%) of HER is necessary to obtain a good quality nickel deposit.

(3) In alkaline ammonia solution, a small amount of cobalt ions improve the quality and color of the deposit, irrespective of the deposition technique used. The yellowish shine of the nickel coating disappears. Therefore, in the possible application, the nickel and cobalt codeposition should be considered.

## Acknowledgments

The authors are grateful to Dr. Eng. Wojciech Nowak for the realization of GD–OES and XRF spectral measurements and to Dr. Eng. M. Wierzbńska for the realization of SEM and EDS measurements.

## References

- [1] YEAGER J, CELS J P, YEAGER E, HOVORKA F. The electrochemistry of nickel. I: Codeposition of nickel and hydrogen from simple aqueous solution [J]. *Journal of the Electrochemical Society*, 1959, 106: 328–336.
- [2] EPELBOIN I, WIART R. Mechanism of electrocrystallization of nickel and cobalt in acidic solution [J]. *Journal of the Electrochemical Society*, 1971, 118: 1577–1582.
- [3] KOLLIA C, SPYRELLYS N, AMBLARD J, FROMENT M, MAURIN G. Nickel plating by pulse electrolysis: Textural and microstructural modification due to adsorption/desorption phenomena [J]. *Journal of Applied Electrochemistry*, 1990, 20: 1025–1032.
- [4] XU W C, DAI P Q, WU X L. Deformation behaviour of electrodeposited nanocrystalline Ni with broad grain size distribution [J]. *Materials Science and Technology*, 2010, 26: 591–596.
- [5] VAZQUEZ-ARENAS J, ALTAMIRANO-GARCIA L, PRITZKER M, LUNA-SANCHEZ R, CABRERA-SIERRA R. Experimental and modeling study of nickel electrodeposition including H<sup>+</sup> and water reduction and homogeneous reactions [J]. *Journal of the Electrochemical Society*, 2011, 158: D33–D41.
- [6] ROSE I, WHITTINGTON C. Nickel plating handbook [M]. Brussels: Nickel Institute, 2014.
- [7] ZHOU Ke-chao, MA Li, LI Zhi-you. Oxidation behaviors of electrodeposited nickel–cobalt coatings in air at 960 °C [J]. *Transactions of Nonferrous Metals Society of China*, 2011, 21: 1052–1060.
- [8] VAZQUEZ-ARENAS J, PRITZKER M. Steady-state model for anomalous Co–Ni electrodeposition in sulfate solutions [J]. *Electrochimica Acta*, 2012, 66: 139–150.
- [9] VAZQUEZ-ARENAS J, ALTAMIRANO-GARCIA L, TREERA-TANAPHITAK T, PRITZKER M, LUNA-SANCHEZ R, CABRERA-SIERRA R. Co–Ni alloy electrodeposition under different conditions of pH, current and composition [J]. *Electrochimica Acta*, 2012, 65: 234–243.
- [10] WU Z W, LEI Y P, WANG Y, FU H G. Effect of cobalt content on microstructure and property of electroplated nickel–cobalt alloy coatings [J]. *Materials Science and Technology*, 2013, 44: 593–600.
- [11] LIU Xue-wu, XU Yun-hua, QU Yi, SUN Li-long. Structure, morphology and wear resistance of electrodeposited Ni–Co alloy deposits [J]. *Integrated Ferroelectrics*, 2014, 152: 144–151.
- [12] LEWIS D B, LEHMBERG C E, MARSHALL G W. The structure and texture development of Ni alloy electrodeposits. III: Nickel–zinc electrodeposits [J]. *Transactions of the Institute of Metal Finishing*, 2004, 82: 64–70.
- [13] FASHU S, GU Chang-dong, ZHANG Jia-lei, HUANG Mei-ling, WANG Xiu-li, TU Jiang-ping. Effect of EDTA and NH<sub>4</sub>Cl additives on electrodeposition of Zn–Ni films from choline chloride-based ionic liquid [J]. *Transactions of Nonferrous Metals Society of China*, 2015, 25: 2054–2064.
- [14] MA Li, ZHANG Long, LI Xiao-bing, LI Zhi-you, ZHOU Ke-chao. Fabrication and characterization of electrodeposited nanocrystalline Ni–Fe alloys for NiFe<sub>2</sub>O<sub>4</sub> spinel coatings [J]. *Transactions of Nonferrous Metals Society of China*, 2015, 25: 146–153.
- [15] HE Mei-feng, WANG Hao, JIANG Hong, ZHAO Su, PAN Deng. Effect of hydrogen peroxide concentration on surface properties of Ni–Cr alloys [J]. *Transactions of Nonferrous Metals Society of China*, 2016, 26: 1353–1358.
- [16] ZHOU Yue-bo, ZHANG Hai-jun. Effect of annealing treatment on cyclic-oxidation of electrodeposited Ni–Al nanocomposite [J]. *Transactions of Nonferrous Metals Society of China*, 2011, 21: 322–329.
- [17] LI Jian-mei, ZHANG Zhao, LI Jin-feng, XUE Min-zhao, LIU Yan-gang. Effect of boron/phosphorus-containing additives on electrodeposited CoNiFe soft magnetic thin films [J]. *Transactions of Nonferrous Metals Society of China*, 2013, 23: 674–680.
- [18] NIU Te, CHEN Wei-wei, CHENG Huan-wu, WANG Lu. Grain growth and thermal stability of nanocrystalline Ni–TiO<sub>2</sub> composites [J]. *Transactions of Nonferrous Metals Society of China*, 2017, 27: 2300–2309.
- [19] ZHU Xu-bei, CAI Chao, ZHENG Guo-qu, ZHANG Zhao, LI Jin-feng. Electrodeposition and corrosion behavior of nanostructured Ni–TiN composite films [J]. *Transactions of Nonferrous Metals Society of China*, 2011, 21: 2216–2224.
- [20] GABE D R. The role of hydrogen in metal electrodeposition processes [J]. *Journal of Applied Electrochemistry*, 1997, 27: 908–915.
- [21] ZHENG Guo-qu, ZHENG Li-feng, CAO Hua-zhen, GAO Zhi-feng, NI Si-yu, ZHANG Jiu-yuan. Nickel electrodeposition from leaching solution containing ammonia and chloride [J]. *Transactions of Nonferrous Metals Society of China*, 2003, 13: 217–220.
- [22] ZHENG Guo-qu, ZHENG Li-feng, CAO Hua-zhen. Formation of black nickel in leaching solution containing ammonia and chloride [J]. *Transactions of Nonferrous Metals Society of China*, 2005, 15: 165–170.
- [23] GRUJICIC D, PESIC B. Electrochemical and AFM study of nickel nucleation mechanisms on vitreous carbon from ammonium sulfate solutions [J]. *Electrochimica Acta*, 2006, 51: 2678–2690.
- [24] RODRIGUEZ-TORRES I, VALENTIN G, LAPICQUE F. Electrodeposition of zinc–nickel alloys from ammonia-containing baths [J]. *Journal of Applied Electrochemistry*, 1999, 29: 1035–1044.

- [25] MOY P W, DU ROSE A H. Alkaline nickel plating solutions: US patent, 2773818 [P]. 1956–12–11.
- [26] ROSE A H D, STERN R L. Alkaline nickel plating solutions: US patent, 3634210 [P]. 1972–01–11.
- [27] ROSE A H D, STERN R L. Alkaline nickel plating solutions: US patent, 3718549 [P]. 1973–02–27.
- [28] ROSE A H D, STERN R L. Alkaline nickel plating solutions: US patent, 3759803 [P]. 1973–10–18.
- [29] INCZÉDY J. Analytical applications of complex equilibria [M]. New York: Halsted Press, 1976.
- [30] HU Chi-chang, WU Chi-ming. Effects of deposition modes on the microstructure of copper deposits from an acidic sulfate bath [J]. Surface and Coatings Technology, 2003, 176: 75–83.
- [31] SKITAŁ P, SANECKI P, GIBAŁA K. The description of the copper deposition/dissolution process in ammonia buffer with the application of mathematical two-plate model [J]. Electrochimica Acta, 2014, 138: 383–391.
- [32] SKITAŁ P, SANECKI P. Developments in electrochemistry [M]. Rijeka, Croatia: InTech, 2012: 29–54.

## 从碱性 $\text{NH}_4\text{OH}/\text{NH}_4\text{Cl}$ 缓冲溶液中电沉积镍

Piotr M. SKITAŁ, Przemysław T. SANECKI, Dorota SALETNIK, Jan KALEMBKIEWICZ

Faculty of Chemistry, Rzeszów University of Technology, 35-959 Rzeszów, Poland

**摘要:** 采用循环伏安、计时电势、计时电流以及光学数码显微镜、辉光放电光谱(GD-OES)、X 射线荧光光谱分析(XRF)、扫描电镜能谱(SEM-EDS)等技术, 研究碱性  $\text{NH}_4\text{OH}/\text{NH}_4\text{Cl}$  缓冲溶液中镍在钢和铜上的电沉积, 目的是从弱碱性溶液中获得镍镀层, 并优化工艺过程。以镍镀层质量为指标, 对电解液组成、pH、温度、电流、电势等工艺参数进行优化。讨论析氢在电沉积过程中的作用, 并研究 Co 作为添加剂的影响。发现少量的 Co 可以催化 Ni 沉积过程、改善镀层的质量和颜色。因此, 在可能的应用中, 应认真考虑 Ni/Co 共沉积。研究还表明, 对于恒电流沉积模式, 镀层的质量与极化电势区间的宽度有关, 此电势区间宽度由计时电势曲线  $E=f(t)$  在沉积过程刚开始时的部分确定。

**关键词:** 镍; 钴; 电沉积; 氨缓冲溶液

(Edited by Wei-ping CHEN)